Journal of Applied Polymer Science

Characteristics of murta bast fiber reinforced epoxy composites

Ajmal Hussain Barbhuiya,[1] Saad Uddin Choudhury,[2] Kochi Ismail[1]
[1]Department of Chemistry, North-Eastern Hill University, Shillong 793022, India
[2]Department of Chemistry, Cotton College, Guwahati 781001, India
Correspondence to: K. Ismail (E-mail: kismail@nehu.ac.in)

ABSTRACT: The growing global concern over environment protection has led to the application of natural fiber reinforced polymer composites as alternative materials in manufacturing sectors. Various natural fibers are therefore being explored for reinforcement of polymer matrices. In the present work, murta bast fibers of varying length and weight percent are mixed randomly with the epoxy matrix and the composites are prepared from these mixtures by using the hand lay-up method. The composites are characterized on the basis of density, thermal gravimetric analysis, infrared spectroscopy, scanning electron microscopy, tensile strength, flexural strength, compressive strength, impact strength, and Rockwell hardness studies. Tensile, flexural, and compressive moduli of the composites are also determined. The tensile strength of the composite was analyzed in the light of the different analytical models. Composites containing 30 weight % fibers of length 25 or 35 mm have the optimum mechanical properties. Murta bast fiber has the characteristics to become a good natural material for reinforcement. © 2016 Wiley Periodicals, Inc. J. Appl. Polym. Sci. **2016**, *133*, 44142.

KEYWORDS: composites; fibers; properties and characterization; resins; thermogravimetric analysis (TGA)

Received 11 March 2016; accepted 30 June 2016
DOI: 10.1002/app.44142

INTRODUCTION

The growing global concern over the negative impact of human activities on environment has led to consider natural fiber reinforced polymer composites as one of the alternative materials for manufacturing eco-friendly and economically viable products for use in automobile, construction, electrical, sports, packaging, household, etc. sectors. This has given an impetus to the research in the field of polymer composites and researchers are faced with the challenge of bringing out better composite materials. As a result, various natural fibers have been explored for reinforcing polymer matrices.[1–27] The advantages of using natural fibers for reinforcement of polymers are easy availability, renewability, biodegradability, low density, high specific strength, noncorrosive nature, and low cost. In a recent report[28] the fibers extracted from the core of the stems of murta (*Schumannianthus dichotomus*) plants (which is referred as murta core fiber) were used for reinforcing the polymer containing AW106 epoxy resin and HV953U hardener (in the ratio of 2:1 by volume) and the mechanical properties of the resultant polymer composite were characterized. Murta plants are grown in Assam and West Bengal states of India, north-eastern parts of Bangladesh, Myanmar, Thailand, Cambodia, Vietnam, Malaysia, and Philippines. Murta fibers are exclusively used for making various handicraft products and out of these products the mat is very popular in India and Bangladesh. It may be mentioned that only the fibers extracted from the outer layer of the stems of murta (which is referred as murta bast fiber) are used for making handicraft products. There is just one report on murta bast fiber reinforced polymer composite by Akter *et al.*[29] wherein the authors investigated the effect of talc amount on the characteristics of an unsaturated polyester resin reinforced by mats of murta bast fiber. The potential use of murta bast fiber for reinforcement of polymer matrices and the effect of its length and loading on the properties of polymer composites are yet to be investigated in detail. Such an investigation is worth carrying out in view of the significance of natural fiber reinforced polymer composites and their applications in various sectors as already mentioned above. Therefore, in the present article murta bast fiber is characterized first by determining its chemical composition and properties, and then the effect of its length and loading on the various properties of epoxy composite is investigated.

The main disadvantage about using natural fibers for reinforcement is its incompatibility with polymer matrix because of hydrophilicity of fiber and hydrophobicity of polymer, which is overcome by surface modification of the fibers by chemical treatments. Different chemical treatments are used for surface modification and the studies carried out by different research groups[30–40] have established that such chemical treatments improve the mechanical performance of the composites. Among the different methods reported,[30–40] alkali treatment or

mercerization is one of the most commonly used methods and the concentration of sodium hydroxide (NaOH) solution used varied from 0.5% to 10%. In the present study 2% sodium hydroxide (NaOH) is arbitrarily chosen for surface modification of murta bast fiber.

EXPERIMENTAL

Materials

Araldite AW106 epoxy resin and HV953U hardener were procured from a local supplier and used as supplied. Araldite AW106 contains bisphenol A diglycidyl ether with an epoxide equivalent weight equal to 214–221 g eq^{-1}. The hardener HV953U contains *N*-(3-dimethyaminopropyl)−1,3-propylenediamine. Laboratory reagent grade NaOH (S. D. Fine Chemicals, India) was used for treating the fibers.

Extraction and Processing of Fibers

The mature stems of the murta plants were collected and every stem was split lengthwise into four equal parts. From each one-fourth part of the stem the outer portion was separated and soaked in water for about one month which made the manual extraction of the fibers easier. The fibers thus collected were thoroughly washed with water and then boiled for two hours in 2% (w/w) NaOH solution. The fibers, after removing from the NaOH solution, were initially washed with water and finally with distilled water. These fibers were sun dried first, and then kept in an oven at about 60 °C for 24 hours and finally at 100 °C for 2 hours. The treated fibers were cut into required lengths.

Preparation of the Composite

AW106 epoxy resin and HV953U hardener were mixed in a stainless steel container in the ratio of 1:1 by volume and added weighed amount of the chemically treated fibers of chosen length. The contents were then thoroughly mixed by stirring. The lengths of the fiber chosen are 15, 25, 35, and 45 mm. Silicone oil was applied on the inner sides of the mould and then the stirred mixture was cast into the mould of 140 mm × 140 mm × 5 mm size. Releasing the polymer composite from the mould was made easy by applying silicone oil. The mixture was spread uniformly over the mould using a steel roller which also helped to remove any trapped air bubbles. The content was then kept under pressure for 24 hours at room temperature. The sheet was removed from the mould and kept in hot air oven (about 70 °C) for another 24 hours. The prepared composite was cut into equal pieces measuring 140 mm × 25 mm × 5 mm and these pieces were used for carrying out various measurements. The pure polymer matrix was also prepared similarly without adding the fiber to the resin + hardener (1:1) mixture.

Measurements

The densities of the polymer, fiber, and the composites were measured at room temperature (25 ± 0.5 °C) by following the ASTM D792 standard method which is based on the Archimedes' principle. For water absorption test of the polymer and composites, the samples of dimension 75 mm × 25 mm × 5 mm were prepared and then kept in an oven for 24 hours by maintaining the temperature at 80 ± 3 °C. The samples were then cooled in desiccator and immediately their weights were noted. Thereafter the samples were immersed in distilled water for 24 hours. The samples were removed from water one at a time and the surface water was wiped off with a dry cloth and the weights were again noted. From the increase in weight of the soaked sample the % of water absorption was then calculated. The weighing was done in a Mettler Toledo AG245 Electronic Balance. The analysis of the untreated murta fibers for determining the chemical composition was done by the Indian Jute Industries' Research Association, Kolkata, India, by using the reported chemical analysis methods.[41–44] Thermo gravimetric analysis (TGA) was done by using Perkin Elmer STA 6000 Simultaneous Thermal Analyzer. The sample (5 mg) was taken in alumina crucible and the analysis was carried out under nitrogen atmosphere (maintained with a continuous flow rate of 100.0 mL min^{-1}) at a heating rate of 10 °C min^{-1}. JEOL JSM 6360 high-resolution scanning electron microscope (SEM) was used to take the SEM images of fiber and the composites at an accelerating voltage of 20 kV. The samples were sputter coated with a layer of homogenous gold to facilitate dissipation of charge during imaging. The infrared (IR) spectra of the fiber, polymer, and composite were taken in Perkin Elmer Spectrum Two FTIR spectrometer. The sample pellets were made in KBr. Tensile, flexural, and compressive strengths of the samples were measured in a Universal Testing Machine (INSTRON Model 8801) at a test speed of 5 mm/min and gauge length of 50 mm. The Izod impact strength of the samples were measured in a Pendulum Impact Tester (FIE Model IT-30). The Rockwell hardness of the samples were measured in HRL scale in a Digital Rockwell Hardness Tester (FIE Model RASNE-1) by using 1/4 inch steel ball indentor and 60 kg load. The measurements of strengths and hardness were made in the Mechanical Engineering Department of Indian Institute of Technology, Guwahati, India, at room temperature (25 ± 1 °C). Sample specimens for the different measurements were prepared according to the ASTM standards. In the case of density, TGA, water absorption, tensile, flexural, compressive, impact, and hardness tests, the measurements were repeated using three specimens for each of the composite sample. The values of the different properties reported here are the average values.

RESULTS AND DISCUSSION

Characteristics of Fiber and Density

The properties and chemical composition of the bast and core fibers of murta are listed in Table I. The properties and chemical compositions of a few known natural fibers are also given in Table I for the sake of comparison. The experimental density values of the composites are presented in Figure 1. The density of the composites increased with increase in the weight % of the fiber. Composites are found to have higher density than the polymer (1.06 g cm^{-3}) and when the fiber load exceeded 20 weight % the composite density even became slightly higher than the density of the fiber (1.10 g cm^{-3}) indicating thereby that the composites are compact and have negligible void. As can be seen from the SEM images (Figure 2) the treatment of the fiber renders its surface more uneven with formation of pits and such a surface facilitates better cohesion between the fiber and matrix. The cohesive interaction between the fiber and the polymer is also evident from the IR spectra shown in Figure 3.

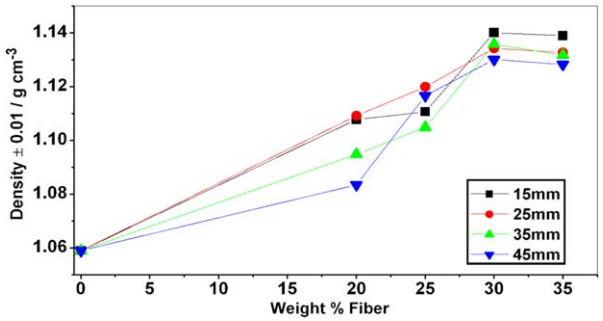

Figure 1. Density of the composite as a function of weight % of fiber of different lengths. [Color figure can be viewed in the online issue, which is available at wileyonlinelibrary.com.]

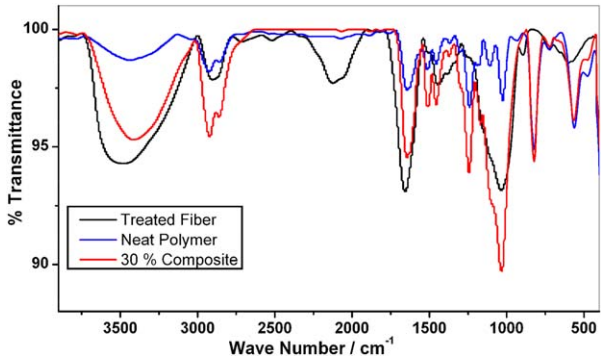

Figure 3. FTIR spectra of the fiber, polymer, and composite (containing 30% fiber). [Color figure can be viewed in the online issue, which is available at wileyonlinelibrary.com.]

In the fiber, the IR band at 3490 cm^{-1} corresponds to OH stretching, whereas in the polymer the IR band at 3450 cm^{-1} corresponds to OH and NH stretching. The increase in intensity and the broadening of the IR band at 3450 cm^{-1} of the polymer on fiber loading confirm that enhancement of hydrogen bonding takes place during formation of composite. The cohesive interaction because of hydrogen bonding between the fiber and the polymer renders compactness to the composite, which probably causes contraction on mixing the polymer and fiber thereby resulting in the increase of density. The density of the composite with 35% fiber loading is slightly lower than that of composite with 30% loading. This may be attributed to agglomeration of fibers causing increase in volume of the composite.

Water Absorption

The water absorption behavior of the composites is shown in Figure 4. The amount of water absorbed by the composite tends to increase with increase in the weight % of fiber and fiber length. The maximum water absorbed is about 14% by the composite with 35 weight % of 45 mm fiber. This appears to be not very high considering the hydrophilic nature of lignocellulosic fibers. For example, jute reinforced polyester composite is reported[4] to have about 25% water absorption.

Thermal Behavior

The thermograms obtained from the TGA are shown in Figure 5 and they illustrate the response of the fiber, polymer, and composites to thermal energy. In the first stage, the fiber loses about 6 weight % near 100 °C. This initial weight loss is considered to be as a result of evaporation of water from the fiber surface, which is a common feature with natural fibers because of their hydrophilic nature. The second stage between 100 and 240 °C is almost a flat region and the fiber loses an additional 1% weight only, which perhaps is because of removal of the internal bound water. In the third stage, the sudden thermal degradation of the fiber begins and continues up to about 350 °C resulting in a weight loss of about 53%. Yang *et al.*[45] isolated hemicellulose, cellulose, and lignin from the palm oil waste samples and determined their individual pyrolysis curves from TGA. Based on these reported[45] thermograms of the three major components of natural fibers, an attempt is made here to calculate the total weight loss of murta fiber at the end of third stage of degradation. From the reported thermograms it is found that at 350 °C temperature the weight losses of hemicellulose, cellulose, and lignin are 63%, 50%, and 25%, respectively. In the light of the composition of murta bast fiber (Table I), at 350 °C the fiber is therefore expected to lose 12%, 28%, and 4% weights because of degradation of hemicellulose (63% of 19%), cellulose (50% of 56%), and lignin (25% of 16%), respectively. The predicted total weight loss of the fiber at 350 °C is then equal to 51% (44% because of degradation of hemicellulose, cellulose, and lignin and 7 weight % because of water evaporation). Interestingly, the weight loss at 350 °C that we obtained from the experimental thermogram shown in Figure 5 is equal

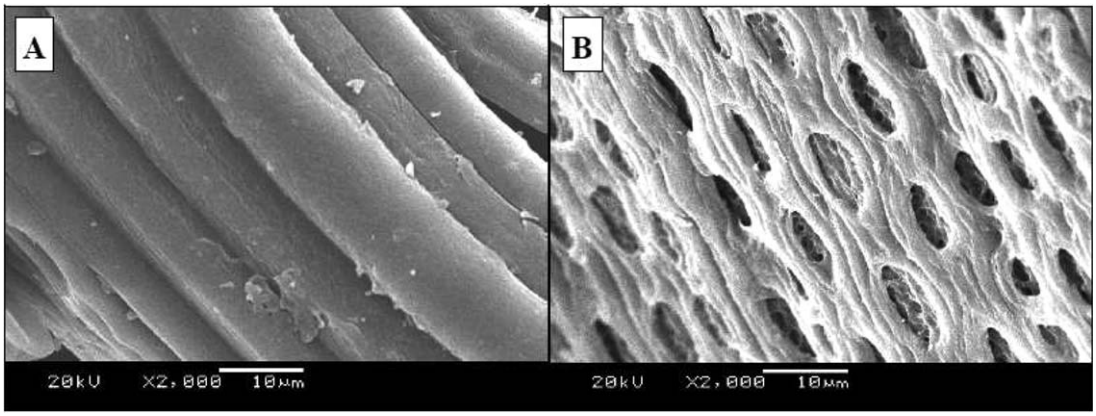

Figure 2. SEM images of (A) untreated and (B) treated fiber.

Table I. Composition and Properties of Murta and Other Fibers

Fiber	Cellulose (%)	Hemi-cellulose (%)	Lignin (%)	Density (g cm^{-3})	TS (MPa)	Ref.
Murta bast fiber	56	19	16	1.10	378 ± 13	Present work
Murta core fiber	38	26	22	0.94	242 ± 24	Present work, 24
Jute	71	20	13	1.3	393-773	21
Sisal	65	12	10	1.5	511-635	21
Coir	43	0.3	45	1.2	175	21
bamboo	26-43	30	21-31	0.8	140-230	1,21
Flax	71	21	2	1.50	345-1035	21
Kenaf	72	20	9		930	21

to 53% which is in good agreement with the predicted value. The fourth stage of thermal degradation of the fiber above 350 °C takes place slowly. According to the TGA results of Yang *et al.*,[45] cellulose undergoes fast degradation in one stage between 315 and 400 °C to lose 95% of its weight, lignin's degradation takes place very slowly from 240 °C onwards (<0.15 weight %/°C) and the degradation of hemicellulose is fast from 220 to 315 °C followed by a very slow degradation (<0.1 weight %/°C). Therefore, the slow thermal degradation of murta fiber in the fourth stage is because of the slow degradation of hemicellulose and lignin. The characteristics of thermal degradation of the polymer and the composites are similar and occur in one fast step. The polymer (epoxy resin to hardner ratio = 1:1) is thermally stable up to 325 °C which is higher than the thermal stability of the polymer with epoxy resin to hardner ratio = 1:2 (293 °C).[28] Although reinforcement by the natural fiber reduces the thermal stability of the polymer matrix, the composites with 30–35 weight % fiber still have thermal stability up to nearly 300 °C.

Tensile Strength and Modulus

The measured tensile strength (TS) of the polymer (33.4 MPa) and composites are shown in Figure 6(A). The TS of a composite is governed by several factors such as length of the fiber, amount of the fiber, orientation of fibers in the matrix, distribution of fibers in the matrix, fiber–matrix adhesion, etc. In the present study, the composites were prepared from the mixtures obtained by mixing the fibers randomly with the polymer matrix, and only length and amount of fiber are used as the variables to monitor the characteristics of the composite. The TS of the composite becomes maximum at a critical length and amount of the fiber and such type of dependence of TS on fiber length and amount is a common feature in natural fiber reinforced composites.[7,10,14] When the composite contains 30 weight % of 35 mm fiber the TS is found to become maximum and is equal to 74.9 MPa, which amounts to an increase of 124% compared to the TS of the neat polymer. It is observed that the composite containing 30 weight % of 25 mm fiber also has nearly maximum TS equal to 74.3 MPa. Beyond 30 weight % fiber load, the TS starts decreasing and this is attributed to agglomeration of the fibers causing discontinuity in the composite and weakening of fiber–matrix adhesion. The SEM images shown in Figure 7 confirm the change in the morphology of the composite containing 35 weight % fiber which envisages agglomeration of fibers.

The tensile stress versus % strain plots for neat polymer and composites are shown in Figure 8. From the stress versus strain plots the tensile modulus (TM) was determined and the values of TM are shown in Figure 6(B). The trend in the variation of TM with weight % of fiber of 15 mm length is found to be different from the general behavior. Barring this exceptional trend in composites containing 15 mm fiber, the variation of TM with fiber load is similar to that of TS. The TM increases with increase in fiber load up to 30 weight % and then starts

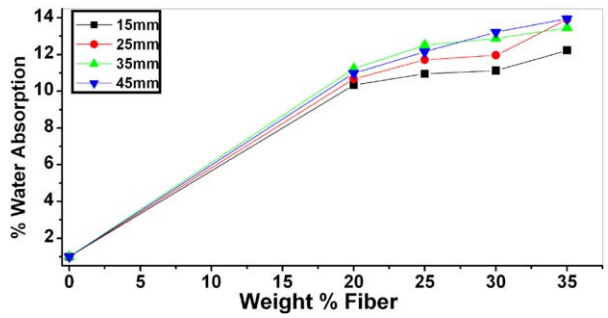

Figure 4. Amount of water absorbed by the composites as a function of weight % of fibers of different lengths. [Color figure can be viewed in the online issue, which is available at wileyonlinelibrary.com.]

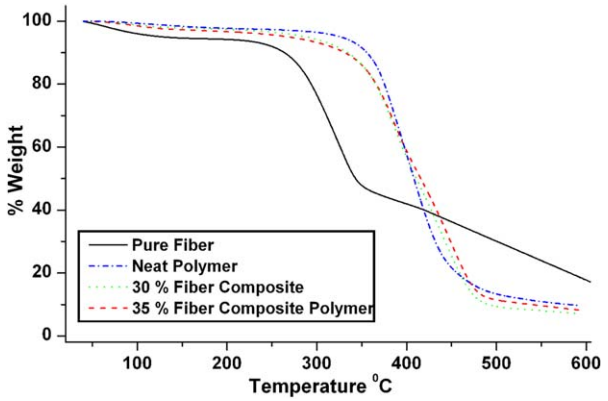

Figure 5. Thermograms of the fiber, polymer, and composites obtained from the TGA. [Color figure can be viewed in the online issue, which is available at wileyonlinelibrary.com.]

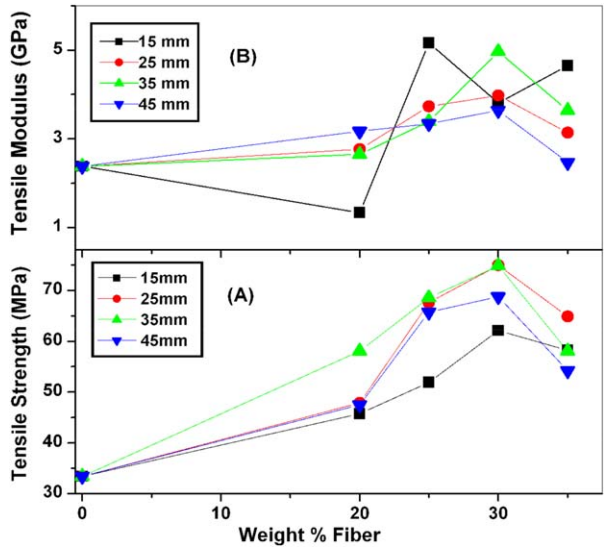

Figure 6. Variation of (A) tensile strength and (B) tensile modulus of the composite as a function of weight % of fiber at fixed fiber lengths. [Color figure can be viewed in the online issue, which is available at wileyonlinelibrary.com.]

decreasing on further increase in the amount of fiber. The highest TM was observed in composite containing 30 weight % of 35 mm fiber. From Figure 8 it becomes obvious that the fiber length plays a significant role in the stress versus strain characteristics of a polymer composite. The % elongation at the break is maximum (6.4%) in the composite containing 30 weight % of 35 mm fiber. The added fiber thus reinforces the polymer matrix by enhancing its strength as well as toughness and therefore in the composite the energy dissipation takes place more effectively.

Flexural Strength and Modulus

Similar to TS, the flexural strength (FS) of the polymer becomes better after fiber loading and FS also attains a maximum value when the composite contains 30 weight % of 35 mm fiber [Figure 9(A)]. The maximum value of FS is 156.6 MPa which is about 69% increase over the FS of neat polymer. Flexural modulus (FM) of the polymer also increases with fiber loading and the composite with 25 weight % of 35 mm fiber has highest FM [Figure 9(B)]. Such observation in which a composite has the highest strength and modulus values corresponding to different weight % of fiber was also reported[10,46] in other natural fiber reinforced polymer composites.

Compressive Strength and Modulus

Compressive strength (CS) values of the composite are shown in Figure 10(A) and CS is found to be maximum when the composite contains 30% fiber, but the fiber length which produces maximum compressive strength is 25 mm and not 30 mm. The CS of the neat polymer is 29.7 MPa and the maximum CS attained by the composite with 25 mm fiber is equal to 78.2 MPa, an enhancement of about 163%. Compressive modulus (CM) values are shown in Figure 10(B). Maximum CM is exhibited by the composite of 30 weight % fiber of length 35 mm.

Figures 6(B), 8, 9(B), and 10(B) reveal that the modulus behavior does not show any clear trend with respect to fiber length and fiber load. Sometimes shortest fiber composites are most stiff, other times they are most compliant. Generally the composites with 35 mm fibers have the best modulus, but there is large variation with respect to loading percentage. One of the probable causes for such irregular trend is that the orientation of the fibers is not controlled in the present composites. After random mixing of fiber and polymer, while laying the mixture on the mould the fibers adopt any orientation which in turn is expected to depend on the fiber population (load) and length.

Impact Strength and Hardness

The impact strength (IS) values of the composites are shown in Figure 11(A) as a function of weight % of fiber. The dependence of IS on fiber length and fiber amount is similar to that of TS, FS, and CS. As in the case of CS, the composite containing 30 weight % of 25 mm fiber has the maximum IS (75.6 J m^{-1}), about 95% more than that of neat fiber (38.8 J m^{-1}). Reinforcement with murta fiber also led to improvement of the hardness of the polymer matrix as shown in Figure 11(B). The maximum hardness (in the HRL scale) is attained by the composite containing 25 weight % of 25 mm fiber (81.9), an increase of about 84% with respect to the hardness of the polymer matrix (44.5). The cohesive interaction between the fiber and polymer because of hydrogen bonding may be responsible for the increase in hardness.

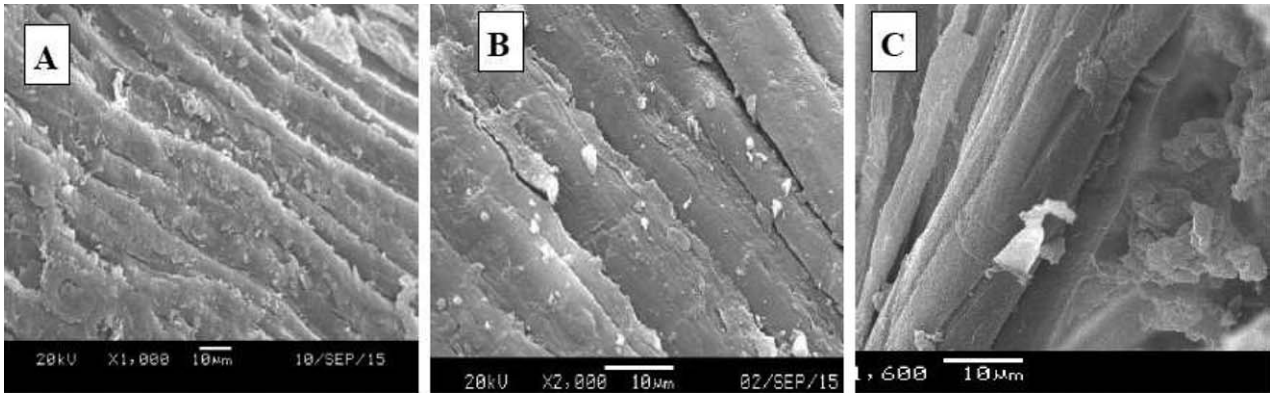

Figure 7. SEM images of composites containing (A) 20%, (B) 25%, and (C) 35% fibers of 35 mm length.

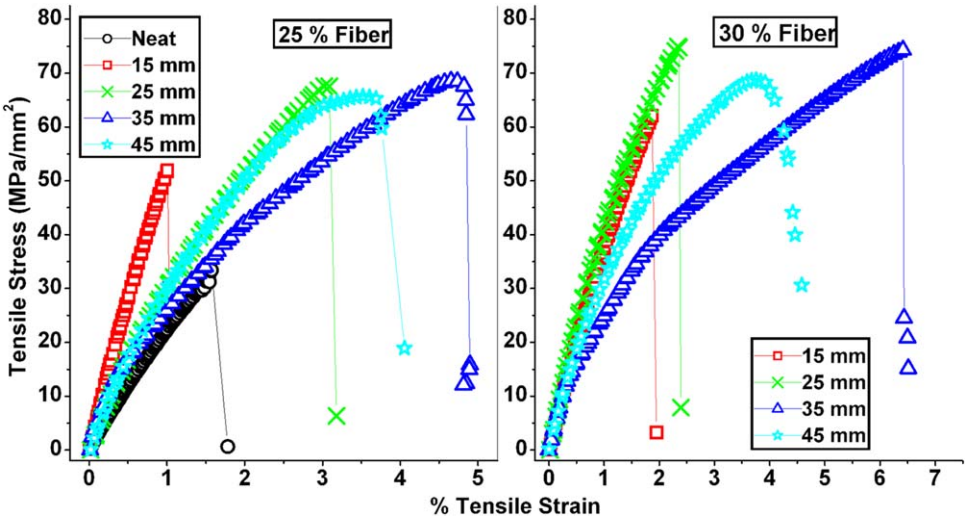

Figure 8. Tensile stress versus % strain plots for neat polymer and composites containing 25 and 30 weight % fiber of varying lengths. [Color figure can be viewed in the online issue, which is available at wileyonlinelibrary.com.]

The behavior of the composite with 35% fiber is found to be quite surprising. All properties of the composite including density and hardness decrease at 35% fiber irrespective of the fiber length. This indicates that the composite of 35% fiber is perhaps not forming well during the fabrication process. The SEM image shown in Figure 7(C) also indicates that in composite of 35% fiber there is agglomeration of the fibers and detachment from the polymer matrix which might be the reason for its poor quality.

Fitting of Tensile Strength Data to Models

An attempt was made to analyze the tensile data of the composites loaded with 25 and 35 mm fibers on the basis of existing theoretical models.[7,47] The first model we applied is the isostrain model, which is also called parallel model. The expression for TS on the basis of this model is written as

$$T_c = T_m V_m + T_f V_f \quad (1)$$

In eq. (1), T and V denote tensile strength and volume fraction, respectively, while the subscripts c, m, and f indicate that the respective property (T or V) is of composite, polymer matrix, and fiber, respectively. The second model we tried is known as the isostress model or the series model and the expression for T_c is given by the relation

$$T_c = \frac{T_m T_f}{T_m V_f + T_f V_m} \quad (2)$$

Equations (1) and (2) are familiarly known as the rule of mixtures and the inverse rule of mixtures, respectively. The volume

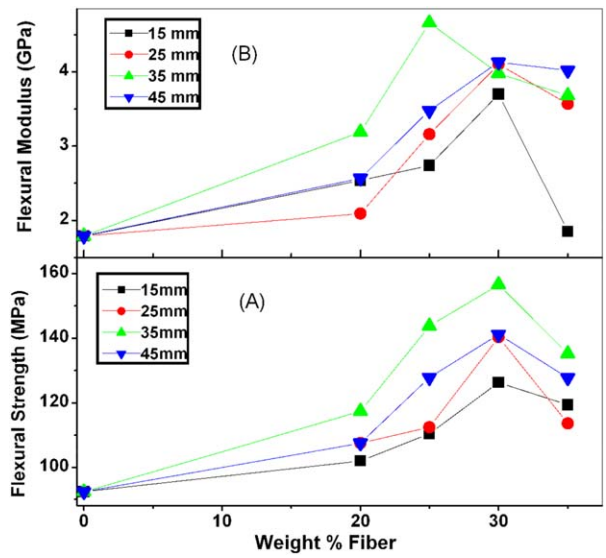

Figure 9. Variation of (A) flexural strength and (B) flexural modulus of the composite as a function of weight % of fiber at fixed fiber lengths. [Color figure can be viewed in the online issue, which is available at wileyonlinelibrary.com.]

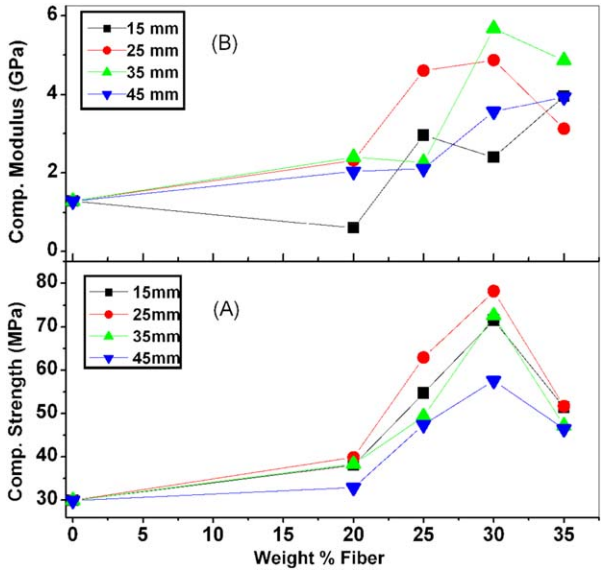

Figure 10. Variation of (A) compressive strength and (B) compressive modulus of the composite as a function of weight % of fiber at fixed fiber lengths. [Color figure can be viewed in the online issue, which is available at wileyonlinelibrary.com.]

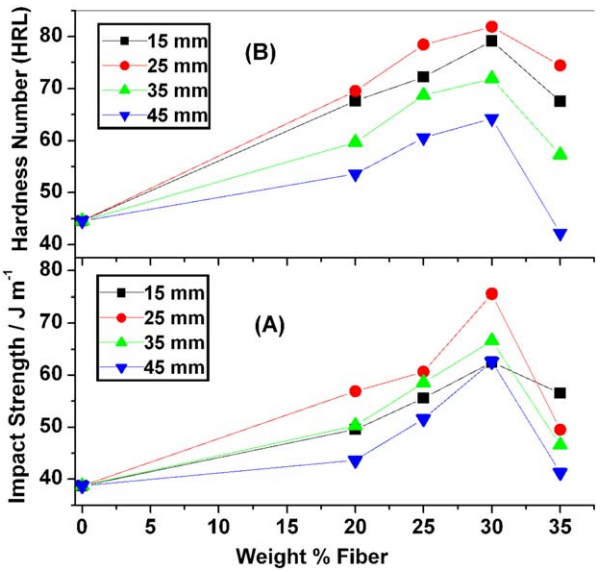

Figure 11. Variation of (A) impact strength and (B) hardness (in HRL scale) of the composite as a function of weight % of fiber at fixed fiber lengths. [Color figure can be viewed in the online issue, which is available at wileyonlinelibrary.com.]

fraction V_f of the fiber in the composite is determined using the relation

$$V_f = \frac{W_f/d_f}{100/d_c} \tag{3}$$

where W_f is the weight % of the fiber, d_f is the density of the fiber, and d_c is the density of the composite. The volume fraction of the matrix V_m is then equal to $1 - V_f$. In the case of eq. (1), it is assumed that isostrain conditions exist for both matrix and fiber, whereas in the case of eq. (2), stress is assumed to be uniform in both matrix and fiber. Moreover, both the eqs. (1) and (2) are for unidirectional fibers. The calculated values of TS from eqs. (1) and (2) are shown in Figure 12. The data do not fit to eq. (1). Although the fit to eq. (2) is much better compared to that to eq. (1), the calculated values from eq. (2) are lower than the experimental values. Thus the assumption of uniform strain (isostrain) does not apply in the present random oriented short-fiber reinforced polymer composite. The assumption of uniform stress (isostress) appears to be nearly, if not fully, applicable to the present composites. We therefore used the Hirsch model,[7] which is a hybrid model as it combines the parallel and series models. According to this model, TS of a composite is expressed by the relation

$$T_c = x(T_m V_m + T_f V_f) + (1-x)\frac{T_m T_f}{T_m V_f + T_f V_m} \tag{4}$$

The value of the coefficient x is determined by fitting the experimental data to eq. (4). The best fits to the experimental values of TS of the composites to eq. (4) were obtained when $x = 0.2$ for 25 mm fiber length and $x = 0.3$ for 35 mm fiber length. Thus, the value of x is controlled by the fiber length. Besides fiber length, factors like fiber orientation and stress transfer from fiber to matrix are also considered to control the value of x. The value of x reveals that the contribution from the series model to the TS of the composite is predominant which supports the inference made above that the tensile property of the composite is governed more by the uniform stress condition. The best fit values of T_c calculated from eq. (4) are shown in Figure 12. The TS data were also analyzed by using the Halpin–Tsai (HT) model.[7,47] The equation based on the HT model is of the form

$$T_c = T_m\left(\frac{1+\alpha\beta V_f}{1-\beta V_f}\right) \tag{5}$$

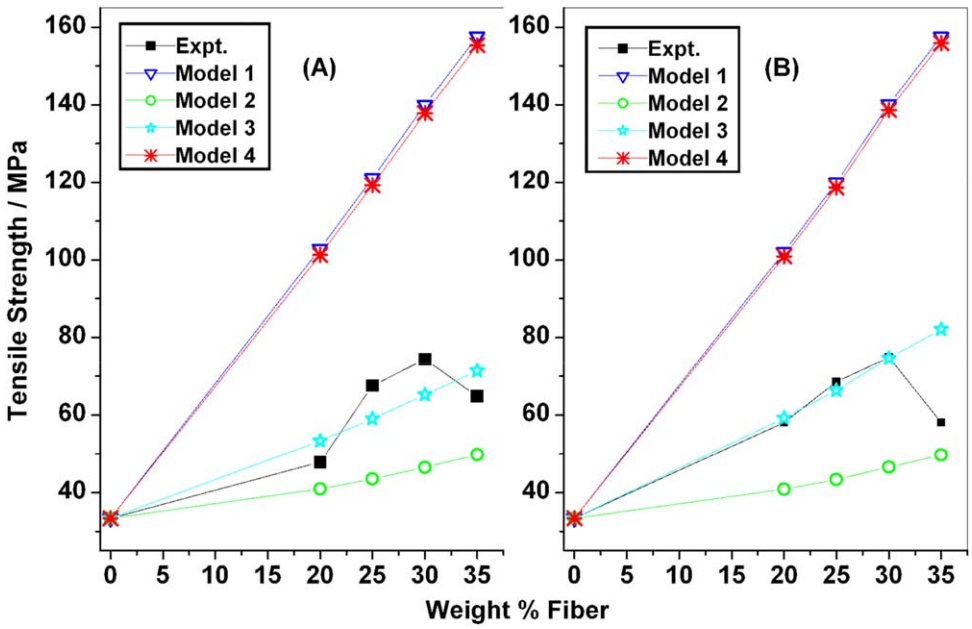

Figure 12. Experimental and fitted values of TS. (A) 25 mm fiber and (B) 35 mm fiber. Equations used for fitting are (i) eq. (1) (Model 1), (ii) eq. (2) (Model 2), (iii) eq. (4) (Model 3), and (iv) eq. (5) (Model 4). [Color figure can be viewed in the online issue, which is available at wileyonlinelibrary.com.]

Table II. Comparison of the Mechanical Strengths of a Few Natural Fiber Reinforced Polymer Composites

Composite					
Polymer	Fiber	Fiber Load (%)[a]	TS (MPa)	FS (MPa)	Ref.
Epoxy		0	33.4	92.4	Present work
	Murta	30 (w)	74.8	156.6	
Polylactic acid		0	62		3
	Kenaf	40 (v)	74	210	3
	Jute	30 (w)	82	—	21
Epoxy		0	24	53	48
	Banana	1 layer of mat	46	74	48
	Toddy Palm	24 (w)	48	—	8
	Jute	35 (v)	66	—	49
	Pineapple Leaf	20 (w)	40	—	50
Poly-propylene		0	28	35	6
	Jute	30 (w)	48	—	21
	Coir	25 (w)	31	57	6

[a]'w' refers to weight % and 'v' refers to volume %.

$$\beta = \frac{(T_f/T_m)-1}{(T_f/T_m)+\alpha} \quad (6)$$

In eq. (5), $\alpha = 2L/D$ where L is the length of the fiber loaded in the matrix and D is the diameter of the fiber used which is equal to 0.14 ± 0.01 mm. The calculated values of TS of the composite using the HT model are very close to those obtained from the Parallel model as can be seen from Figure 12. It can be shown that eq. (5) based on the HT model takes the form of eq. (1) when $L \rightarrow \infty$ and it also takes the form of eq. (2) when $L \rightarrow 0$. Since for fitting we used the experimental data of the composite containing 25 and 35 mm fibers, the corresponding values of α are equal to 357 (for 25 mm) and 500 (for 35 mm) which are very large and almost fulfils the limit $L \rightarrow \infty$. This is the reason for the calculated values of T_c from eqs. (5) to (1) are close to each other. The experimental TS data therefore do not fit into the HT model. It has been observed that to get a good fit the model used must have at least one adjustable parameter. All the models however predict increase of TS with increase in weight % of fiber and the decrease in TS above 30 weight % fiber load cannot be accounted for by any model.

Comparison with Other Composites

Finally, the tensile and flexural strengths of the composite under study were compared with the strengths of a few reported[3,6,21,48–50] polymer composites (Table II). The performance of the murta bast fiber in reinforcing polymer matrix appears to be quite comparable to that of commonly used natural fibers.

CONCLUSIONS

Treated murta bast fiber reinforced epoxy composites are characterized and the tensile strength was analyzed using the known theoretical models. Only those models having at least one adjustable parameter are able to give good fit to the tensile data. The composite attains optimum strength and toughness when the fiber load is 30 weight % and fiber length is 35 mm. Impact strength and hardness however become optimum with 30 weight % of 25 mm fiber. Murta fiber undoubtedly improves the strength and toughness of the polymer matrix, and hence can be a viable bio-material for reinforcement of polymer matrices.

ACKNOWLEDGMENTS

The authors are thankful to the Head, Department of Mechanical Engineering, Indian Institute of Technology, Guwahati, India for providing instrumental facilities to test the composite samples.

REFERENCES

1. Nuthong, W.; Uawongsuwan, P.; Pivsa-Arta, W.; Hamada, H. *Energy Procedia* **2013**, *34*, 839.
2. Naveenkumar, R.; Sharun, V.; Dhanasakkaravarthi, B.; Rajakumar, I. P. T. *Int. J. Appl. Sci. Eng. Res.* **2015**, *4*, 250.
3. Ngo, W. L.; Pang, M. M.; Yong, L. C.; Tshai, K. Y. *Adv. Environ. Biol.* **2014**, *8*, 2742.
4. Ramesh, M.; Palanikumar, K.; Reddy, K. H. *J. Appl. Polym. Sci.* **2016**, *133*, DOI: 10.1002/app.42968.
5. Koradiya, S. B.; Patel, J. P.; Parsania, P. H. *Polym. Plast. Technol. Eng.* **2010**, *49*, 1445.
6. Begum, K.; Islam, M. A.; Huque, M. M. *J. Sci. Res.* **2015**, *7*, 97.
7. Kalaprasad, G.; Joseph, K.; Thomas, S.; Pavithran, C. *J. Mater. Sci.* **1997**, *32*, 4261.
8. Reddy, K. O.; Maheswari, C. U.; Reddy, K. R.; Shukla, M.; Muzenda, E.; Rajulu, A. V. *Int. J. Polym. Anal. Charact.* **2015**, *20*, 612.

9. Xia, G.; Reddy, K. O.; Maheswari, C. U.; Jayaramudu, J.; Zhang, J.; Zhang, J.; Rajulu, A. V. *Int. J. Polym. Anal. Charact.* **2015**, *20*, 377.
10. Shibata, M.; Takachiyo, K. I.; Ozawa, K.; Yosomiya, R.; Takeishi, H. *J. Appl. Polym. Sci.* **2002**, *85*, 129.
11. Marques, M. F. V.; Lunz, J. N.; Aguiar, V. O.; Grafova, I.; Kemell, M.; Visentin, F.; Sartori, A. Grafov *J. Polym. Environ.* **2015**, *23*, 251.
12. Monteiro, S. N.; Calado, V.; Rodriguez, R. J. S.; Margem, F. M. *J. Mater. Res. Technol.* **2012**, *1*, 117.
13. Sekaran, A. S. J.; Kumar, K. P.; Pitchandi, K. *Bull. Mater. Sci.* **2015**, *38*, 1183.
14. Thakur, V. K.; Thakur, M. K. *Carbohydr. Polym.* **2014**, *109*, 102.
15. Jawaid, M.; Khalil, H. P. S. A. *Carbohydr. Polym.* **2011**, *86*,
16. Ashik, K. P.; Sharma, R. S. *J. Miner. Mater. Character. Eng.* **2015**, *3*, 420.
17. Loh, Y. R.; Sujan, D.; Rahman, M. E.; Das, C. A. *Resour. Conserv. Recy.* **2013**, *75*, 14.
18. Nguong, C. W.; Lee, S. N. B.; Sujan, D. *Int. J. Chem. Mol. Nucl. Mater. Metall. Eng.* **2013**, *7*, 33.
19. Ku, H.; Wang, H.; Pattarachaiyakoop, N.; Trada, M. *Compos. B* **2011**, *42*, 856.
20. Facca, A. G.; Kortschot, M. T.; Yan, N. *Compos. Sci. Technol.* **2007**, *67*, 2454.
21. Faruk, O.; Bledzki, A. K.; Fink, H. P.; Sain, M. *Prog. Polym. Sci.* **2012**, *37*, 1552.
22. John, M. J.; Thomas, S. *Carbohydr. Polym.* **2008**, *71*, 343.
23. Satyanarayana, K. G.; Arizaga, G. G. C.; Wypych, W. *Prog. Polym. Sci.* **2009**, *34*, 982.
24. Hao, W.; Ge, D.; Ma, Y.; Yao, X.; Shi, Y. *Polym. Test.* **2012**, *31*, 520.
25. Hao, W.; Yuan, Y.; Zhu, J.; Chen, L. *J. Adhes. Sci. Technol.* **2016**, *30*, 1189.
26. Hao, W.; Zhang, Y.; Yuan, Y. *Polym. Test.* **2016**, *50*, 224.
27. Hao, W.; Tang, C.; Yuan, Y.; Yao, X.; Ma, Y. *Polym. Test.* **2015**, *41*, 239.
28. Barbhuiya, A. H.; Ismail, K. *Int. J. Polym. Anal. Charact.* **2016**, *21*, DOI: 10.1080/1023666X.2016.1139282.
29. Akter, R.; Sultana, R.; Alam, M. Z.; Qadir, M. R.; Begum, M. H. A.; Gafur, M. A. *Int. J. Eng. Technol.* **2013**, *13*, 122.
30. Maldas, D.; Kokta, B. V.; Raj, R. G.; Daneault, C. *Polymer* **1988**, *29*, 1255.
31. Maldas, D.; Kokta, B. V. *J. Compos. Mater* **1991**, *25*, 375.
32. Bledzki, A. K.; Reihmane, S.; Gassan, J. *J. Appl. Polym. Sci.* **1996**, *59*, 1329.
33. Joseph, K.; Thomas, S.; Pavithran, C. *Polymer* **1996**, *37*, 5139.
34. George, J.; Bhagawan, S. S.; Thomas, S. *Compos. Interface* **1998**, *5*, 201.
35. Sreekala, M. S.; Kumaran, M. G.; Joseph, S.; Jacob, M.; Thomas, S. *Appl. Compos. Mater.* **2000**, *7*, 295.
36. Dipa, R.; Sarkar, B. K.; Rana, A. K.; Bose, N. R. *Bull. Mater. Sci.* **2001**, *24*, 129.
37. Leonard, Y. M.; Martin, P. A. *J. Appl. Polym. Sci.* **2002**, *84*, 2222.
38. Rout, J.; Misra, M.; Tripathy, S.; Nayak, S. K.; Mohanty, A. K. *Compos. Sci. Technol.* **2001**, *61*, 1303.
39. Tserki, V.; Zafeiropoulos, N. E.; Simon, F.; Panayiotou, C. *Compos. A* **2005**, *36*, 1110.
40. Xue, L.; Lope, G. T.; Satyanarayan, P. J. *Polym. Environ.* **2007**, *15*, 25.
41. Sarkar, P. B.; Chatterjee, H.; Mazumdar, A. K.; Pal, K. B. *J. Text. Inst.* **1948**, *39*, T1.
42. Sarkar, P. B.; Mazumdar, A. K.; Pal, K. B. *J. Text. Inst.* **1948**, *39*, T44.
43. Sengupta, A. B.; Mazumdar, S. K.; Macmillan, N. G. *Indian J. Appl. Chem.* **1958**, *21*, 105.
44. Norman, A. G.; Jenkins, S. H. *Biochem. J.* **1933**, *27*, 818.
45. Yang, H.; Yan, R.; Chen, H.; Zheng, C.; Lee, D. H.; Liang, D. T. *Energy Fuel* **2006**, *20*, 388.
46. Agunsoye, J. O.; Aigbodion, V. S. *Result. Phys.* **2013**, *3*, 187.
47. Facca, A. G.; Kortschot, M. T.; Yan, N. *Compos. A* **2006**, *37*, 1660.
48. Maleque, M. A.; Belal, F. Y.; Sapuan, S. M. *Arab. J. Sci. Eng.* **2007**, *32*, 359.
49. Sarikanat, M. *J. Reinf. Plast. Compos.* **2010**, *29*, 807.
50. Shih, Y. F.; Cai, J. X.; Kuan, C. S.; Hsieh, C. F. *Compos. B* **2012**, *43*, 2817.